Synthetic Metals 215 (2016) 229–234

Contents lists available at ScienceDirect

Synthetic Metals

journal homepage: www.elsevier.com/locate/synmet

Solution-processed star-shaped oligomers in normal and inverted organic solar cells

V.A. Trukhanov[a], A.L. Mannanov[a], I. Burgués-Ceballos[b], A. Savva[b], S.A. Choulis[b], A.N. Solodukhin[c], Yu. N. Luponosov[c], S.A. Ponomarenko[c,d], D.Yu. Paraschuk[a,*]

[a] International Laser Center and Faculty of Physics, Lomonosov Moscow State University, Leninskie gory 1, Moscow 119991, Russia
[b] Molecular Electronics and Photonics Research Unit, Department of Mechanical Engineering and Material Science and Engineering, Cyprus University of Technology, 45 Kitiou Kyprianou, 3041, Limassol, Cyprus
[c] Enikolopov Institute of Polymer Synthetic Materials of RAS, Profsoyuznaya 70, Moscow 117393, Russia
[d] Chemistry Department, Lomonosov Moscow State University, Leninskie Gory 1/3, Moscow 119991, Russia

ARTICLE INFO

Article history:
Received 14 December 2015
Received in revised form 4 February 2016
Accepted 22 February 2016

Keywords:
Small-molecule organic solar cells
Normal and inverted architecture
Star-shaped oligomers

ABSTRACT

The performance of three different star-shaped oligomers (SSOs) as electron donor materials for organic solar cells is investigated. These promising donor components are blended with [6,6]-phenyl-C_{71}-butyric acid methyl ester ($PC_{71}BM$) fullerene acceptor and solution-processed normal and inverted organic solar cells are fabricated. These SSOs are based on a triphenylamine core and differ in the solubilizing groups and the oligothiophene arm length. We have found that the power conversion efficiency (PCE) is by 10–60% higher in the normal structure, mainly due to an enhanced open-circuit voltage and fill factor. The observed difference in device performance can be assigned partly to the lower leakage currents. By using contact angle measurements and atomic-force microscopy studies, we estimate the degree of vertical phase separation in bulk heterojunctions. The latter has a good correlation to the corresponding photocurrent differences obtained in the normal and inverted structure devices.

1. Introduction

Small molecule donor materials are perspective competitors of conjugated polymers in organic solar cells due to their well-defined molecular structure and molecular weight, better reproducibility and easier purification [1]. Moreover, the record power conversion efficiency (PCE) of organic solar cells was achieved with the use of small molecular donors [2]. Among them, the star-shaped oligomers (SSO) with a triphenylamine core and dicyanovynil acceptor groups are promising donor materials for solution-processed organic photovoltaics [3]. For a recent few years, a number of SSO with various solubilizing groups and different lengths of the oligothiophene arms have been synthesized and studied in organic solar cells [4–6]. Some SSO can form various columnar mesophases [7], which can be used to control the bulk heterojunctions morphology. A PCE higher than 5% was reported for SSO in the normal structure of organic solar cells, where high and low work-function electrodes are at the bottom and the top of the active layer, respectively [8]. On the other hand, the inverted structure, in which the high work-function electrode is on the top and the low work-function electrode is at the bottom of the active layer, usually provides higher air stability, which is crucial for practical applications [9–12]. However, the photovoltaic performance can differ from normal to inverted structure due to several reasons. For example, the vertical separation of the donor and acceptor phases may occur in the active layer upon film formation [13]. If the donor phase is concentrated at the bottom (top) of the active layer, the normal (inverted) structure is more (less) preferential for efficient collection of the photogenerated charges. Moreover, the different electrode and interface materials used in the normal and inverted structures can affect the cell performance. Therefore, both structures deserve comparing when studying novel materials for bulk heterojunction solar cells.

Among the SSO-based organic solar cells, the SSO N(Ph-2T-DCV-Et)$_3$ (Fig. 1, referenced below as SSO1) was compared in a previous work in normal and inverted structures. The photovoltaic performance was virtually the same for both architectures with a PCE of around 3–4% [14]. Interestingly, the different chemical moieties within the SSO1 molecule allowed using green solvents for its processing, leading to comparable photovoltaic performances as with halogenated solvents [15]. It was also found that small solubilizing groups at the SSO branch endings are beneficial

* Corresponding author.
E-mail address: paras@physics.msu.ru (D.Y. Paraschuk).

http://dx.doi.org/10.1016/j.synthmet.2016.02.022
0379-6779/

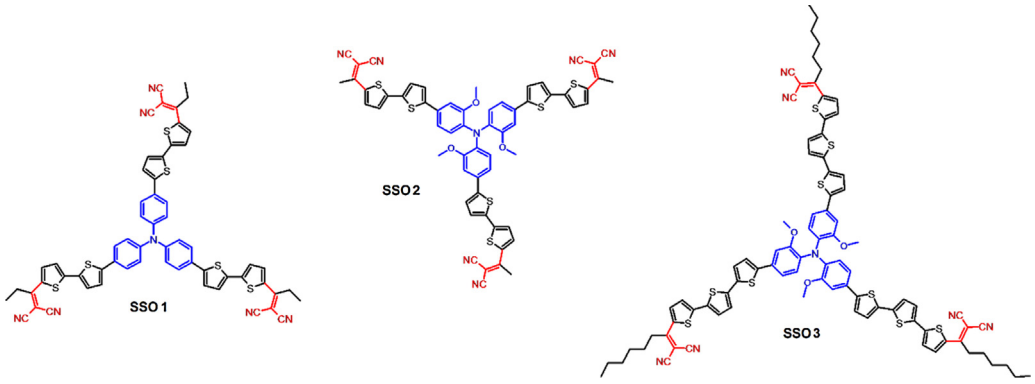

Fig. 1. Structural formulas of studied star-shaped oligothiophenes SSO1-3.

for the photovoltaic performance but result in limited solubility, whereas the bulky solubilizing groups increase solubility but limit the PCE [7]. To achieve a proper balance between an acceptable solubility and high photovoltaic performance, it was suggested to attach solubilizing groups to the SSO interior, specifically methoxy groups at the triphenylamine core [16]. A SSO with methoxy groups, N(Ph(OMe)-2T-DCV-Me)$_3$ (Fig. 1, further designated as SSO2), was synthesized and tested in the normal structure of bulk heterojunction solar cells [16], but its PCE did not outperform that of SSO1. One of the possible reasons for the lower SSO2 performance could be an unsuitable vertical separation of the SSO and PCBM phases in the active layer. To investigate this, normal and inverted architectures should be compared. Moreover, methoxy-substitution at the triphenylamine core resulted in acceptable solubility for the SSO with longer oligothiophene arms and lead to a columnar mesophase [7] in films of N(Ph(OMe)-3T-DCV-Hex)$_3$ (Fig. 1, referenced below as SSO3) [17]. All in all, the recent advances in the SSO-based solution-processed photovoltaics together with the mentioned morphological uncertainties motivate us to compare the normal and inverted structures of SSO-PCBM organic solar cells.

In this work, we compare the photovoltaic performance of organic solar cells based on the three SSO depicted in Fig. 1 in normal and inverted structures. We have found that the PCE is higher in the normal structure and analyzed possible reasons of the lower performance of the inverted solar cells.

2. Experimental

Fig. 1 shows the chemical structures of the studied SSO, which were synthesized using the recently developed approach presented in Refs. [5,7]. The solubilities of SSO1, SSO2 and SSO3 in o-dichlorobenzene are 8 g/l, 14 g/l and 15 g/l, respectively [7,16,17]. $PC_{71}BM$ of 99% purity was purchased from Solenne.

Fig. 2 presents the schematic structures of normal and inverted organic solar cells. The set of organic solar cell devices were fabricated in the following way. First, glass substrates coated with a patterned indium-tin oxide (ITO) layer were cleaned in an ultrasonic bath and treated in an ultraviolet photoreactor. Then, for normal structure devices, a 50-nm-thick layer of poly(3,4-ethylenedioxythiophene):poly(styrene sulfonate) (PEDOT:PSS) was deposited on the ITO and annealed at 140 °C for 15 min. For inverted structure devices, a 40-nm thick ZnO layer was deposited on the ITO using a sol-gel method [18]. Solutions of the SSO:$PC_{71}BM$ blend (mass ratio 1:2) in o-dichlorobenzene with a total concentration of 27 g/l were prepared and stirred overnight at 75 °C prior to deposition. The active layer was deposited in air conditions by doctor-blading, yielding a thickness of 50–60 nm in all the cases. On top of the active layer, a top electrode consisting of Ca/Al (MoO_3/Ag) for the normal (inverted) structure was evaporated in a vacuum chamber. The active area (S) of each device, defined through a shadow mask, was 9 mm^2. Current-voltage characteristics of the devices were measured using a source-meter (Keithley SourceMeter 2400) in dark and under AM1.5G irradiation with an intensity of 100 mW/cm^2. Contact angle measurements (DataPhysics OCA 15EC) were performed on the films without top electrodes using a 1–2 mm-diameter drop of deionized water on top of the film.

3. Results and discussion

Fig. 3 shows current-voltage (J-V) characteristics under simulated solar light and in dark conditions for the best normal and inverted solar cells of each SSO. Fig. 4 compares maximum and

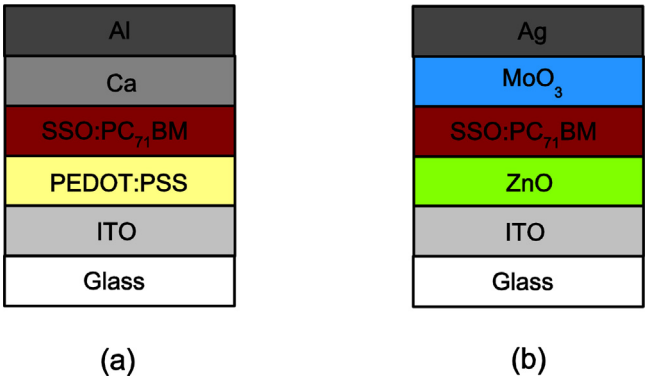

Fig. 2. Normal (a) and inverted (b) device structures of SSO-based organic solar cells.

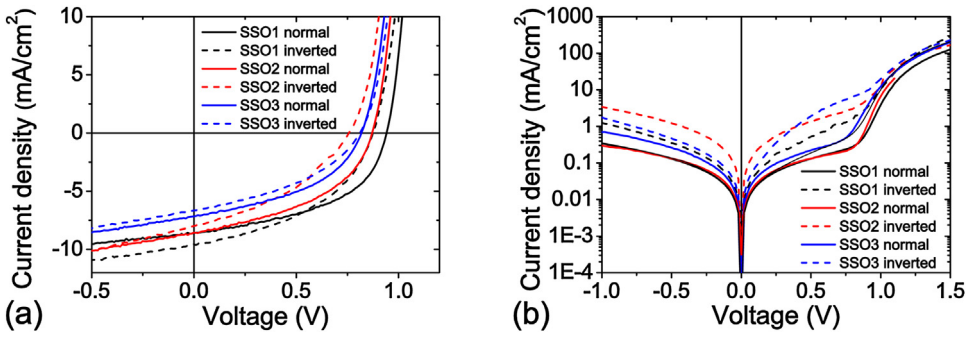

Fig. 3. J-V characteristics of the best SSO-$PC_{71}BM$ solar cells in the normal and inverted structures under illumination (a) and typical J-V characteristics in dark conditions (b).

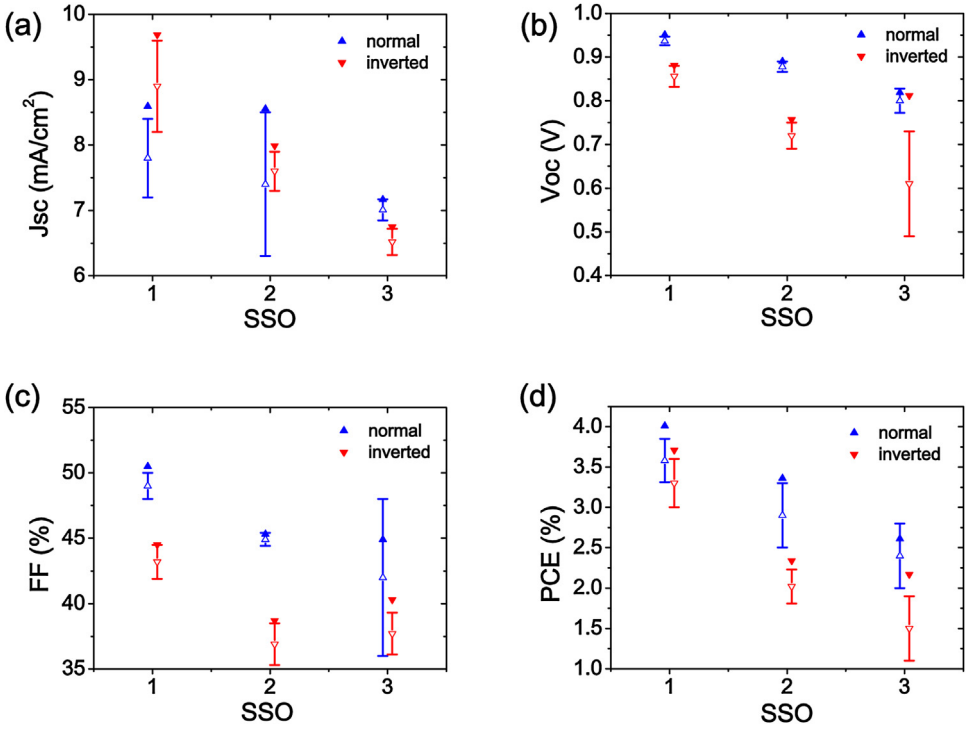

Fig. 4. Maximum (filled triangles) and average (unfilled triangles) J_{SC} (a), V_{OC} (b), FF (c) and PCE (d) for SSO-$PC_{71}BM$ solar cells in the normal and inverted structures.

Table 1
Maximum photovoltaic parameters and average series and shunt resistances of SSO-based normal and inverted solar cells.

SSO	Structure	J_{SC}, mA/cm²	V_{OC}, V	FF, %	PCE, %	R_{ser}, Ohm	$R_{sh}S$, kOhm cm²
1	normal	8.59	0.942	49.5	4.01	24 ± 6	4.3 ± 1.2
	inverted	9.55	0.875	44.5	3.71	10 ± 4	1.8 ± 0.4
2	normal	8.56	0.871	45.1	3.36	23 ± 6	4.1 ± 1.7
	inverted	7.99	0.757	38.8	2.35	12 ± 4	0.7 ± 0.5
3	normal	7.17	0.819	44.5	2.61	20 ± 7	2.5 ± 0.5
	inverted	6.65	0.812	40.3	2.17	15 ± 7	1.9 ± 1.4

average values of short-circuit current density (J_{SC}), open circuit voltage (V_{OC}), fill-factor (FF), and PCE. Table 1 shows numerical values of maximum photovoltaic parameters (the numerical data for average photovoltaic parameters are given in Table S1 of Supporting information). For SSO1, the average and maximum J_{SC} are about 10% higher in the inverted structure than in the normal one, they are virtually the same in both structures for SSO2, and for SSO3 J_{SC} are higher in the normal structure. On the other hand, the rest of photovoltaic parameters (V_{OC}, FF and PCE) are higher in the normal structure. Below we analyze possible reasons for such differences in the photovoltaic performance.

In Table 1 the average values of series resistance R_{ser} and shunt resistance per area $R_{sh}S$ for the normal and inverted SSO-based cells are given. R_{ser} and R_{sh} were calculated over several devices from linear approximation of the dark current voltage characteristics presented in Fig. 3b at high voltages and near zero voltage, respectively. The lower R_{ser} for inverted structure can be assigned to an improved contact between the anode and the active layer

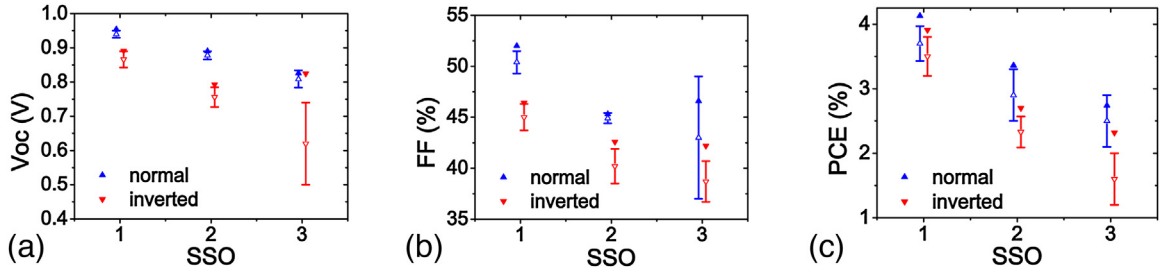

Fig. 5. Maximum (filled triangles) and average (unfilled triangles) V_{OC} (a), FF (b) and PCE (c) for SSO-$PC_{71}BM$ solar cells in the normal and inverted structures after subtraction of the leakage currents V/R_{sh}.

because of better alignment of the SSO highest occupied molecular orbital [14,16,17] with MoO_3 [19] than with PEDOT:PSS [20].

We ascribe the lower shunt resistances R_{sh} for the inverted cells to a lower homogeneity of the active layer film resulting from its deposition on the rougher ZnO surface [18] compared to PEDOT:PSS. These shunts in the inverted structure, especially for SSO2, can be the origin of the lower V_{OC} and FF. To estimate the impact of shunts on the photovoltaic parameters, the shunt current V/R_{sh} was subtracted from the J-V characteristics under light. Fig. 5 shows the photovoltaic parameters calculated from these J-V characteristics. Although V_{OC} and FF increased for the inverted structure, they are still below the values for the normal structure. Thus, we conclude that the shunts are not the only reason for the lower V_{OC} and FF for the inverted SSO-$PC_{71}BM$ solar cells.

The other possible reason of the lower performance of SSO in the inverted structure could be an insufficiently high Fermi level of the electron-injecting electrode (ZnO), which is about −4.4 eV, compared to −2.7 eV for calcium in the normal structure. This would lead to a lowered energy difference between the hole and electron quasi-Fermi levels, which would result in a decreased V_{OC} and FF.

During the formation of the active layer, vertical separation of the donor and acceptor phases may occur. As a result, the donor-acceptor ratio can vary along the normal to the active layer. A strong undesirable vertical phase separation, where the donor prevails near cathode and (or) the acceptor prevails near anode, can decrease number of collected photogenerated charges, PCE and specifically J_{SC}. To estimate whether the differences in J_{SC} in the normal and inverted structures are caused by the vertical phase separation, we investigated the active layer surface in comparison with layers of the pristine donor and acceptor using atomic-force microscopy and contact angle measurements.

Fig. 6 summarizes the results of contact angle measurement on surfaces of pristine SSO1–SSO3, $PC_{71}BM$ and their blends (the numerical data are presented in Table S2 of Supporting information). As vertical phase separation can depend on the wetting properties of the underlayer on which the active layer is deposited, two different underlying layers were used: polymer (PEDOT:PSS) and metal-oxide (ITO). The former is used in the normal structure devices, and the wetting properties of the latter are supposed to be similar to ZnO used in the inverted devices. On pristine SSO layers, the contact angle systematically increases with the number of CH units in alkyl and alkoxy groups in the SSO structure, regardless of the underlayer. This seemingly reflects the tendency of alkyl and alkoxy groups to remain at the film surface to decrease its surface energy.

The contact angles on SSO1:$PC_{71}BM$ blends casted on both underlayers are close to those of pristine SSO1 (Fig. 6). This indicates that, despite of twice higher content of $PC_{71}BM$, the donor content is higher at the top of the active layer, and hence it is assumed to be more beneficial for the inverted structure. This is in line with the higher J_{SC} measured for the inverted solar cells as compared to the normal ones (Fig. 4a). The contact angles on SSO2:$PC_{71}BM$ blends deposited on both underlayers are between those of the pristine SSO2 and $PC_{71}BM$ layers. Assuming similar donor-acceptor ratio at the surface and in the bulk, no significant vertical phase separation is expected for this blend. This is in accordance with the obtained photovoltaic data, which show that J_{SC} is almost the same for SSO2:$PC_{71}BM$ blends in both structures (Fig. 4a). For SSO3 and $PC_{71}BM$, the contact angles on pristine layers are very similar for both underlayers (Fig. 6). However, the contact angle on the SSO3:$PC_{71}BM$ blend is closer to that of pristine $PC_{71}BM$. Therefore, it can be deduced that there is more enrichment of $PC_{71}BM$ at the active layer surface, and hence one can expect vertical phase separation preferential for the normal structure. This deduced vertical phase separation is in agreement with the higher J_{SC} for the normal SSO3-based cell (Figs. 4 and 5).

Atomic-force microscopy images of pristine SSOs, $PC_{71}BM$, and SSO:$PC_{71}BM$ active layers (Fig. S1 in Supporting information) show that the blend morphology is somewhat average between those of

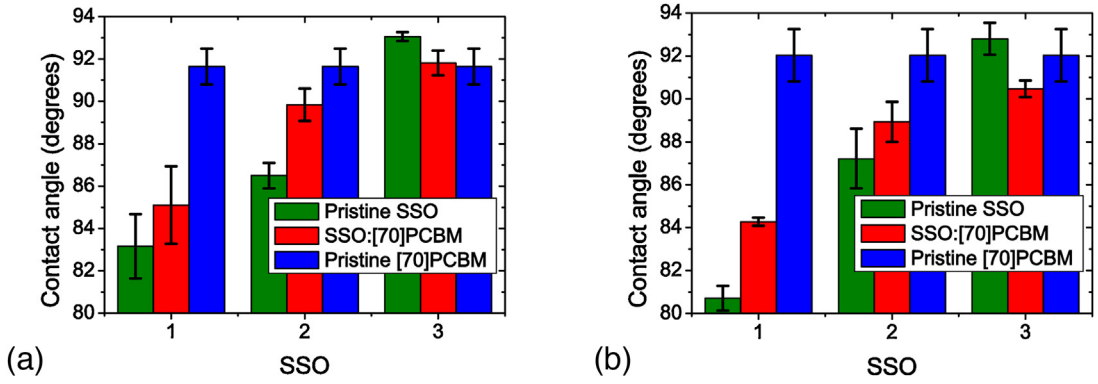

Fig. 6. Contact angles of deionized water on top of surfaces of pristine donor (SSO) and acceptor ($PC_{71}BM$) components and of their blend (SSO:$PC_{71}BM$). The active layers were deposited on PEDOT:PSS (a) or on ITO (b).

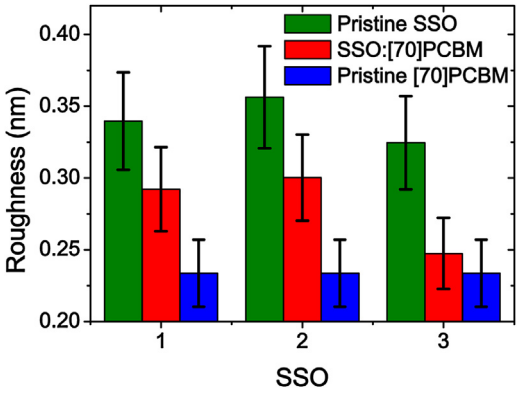

Fig. 7. Average roughness R_a of surfaces of pristine donor (SSO) and acceptor ($PC_{71}BM$) components and of their blend (SSO:$PC_{71}BM$).

the pristine SSOs and $PC_{71}BM$. As Fig. 7 shows, the average roughness, R_a, for the SSO1 and SSO2 blends is between those of the pristine components, whereas R_a for the SSO3 blend is very close to that of $PC_{71}BM$. We can suppose that this roughness results from a higher $PC_{71}BM$ content, which is in accordance with the above contact angle and photovoltaic data.

We speculate that opposite differences in J_{SC} for the normal and inverted device structures of SSO1 and SSO3-based solar cells can be associated with opposite vertical phase separation of the active layer components. This is in line with the series resistances (Table 1) that in row SSO1-SSO2-SSO3 show a weak tendency to decrease for normal and increase for the inverted devices as the vertical phase separation results in different contact areas of donor and acceptor with the electrodes. Nevertheless, the observed differences in J_{SC} can also result from other reasons, e.g. differences in interface recombination at the electrode contacts and in the optical spacing effect. A deeper analysis of these reasons would deserve a separate study.

4. Conclusions

Three different star-shaped oligomer-based organic solar cells were compared in both normal and inverted solar cells architectures. The normal structure results in better photovoltaic performance, mainly due to the higher open-circuit voltage and fill factor values. We suggest that the latter are lower in the inverted structure partly due to shunts. Further analysis has been performed to elucidate the eventual influence of vertical phase separation of the active layer on the device performance. The results of contact angle measurements and atomic force microscopy on the different SSO:$PC_{71}BM$ active layers correlate with the different short-circuit currents obtained in the normal and inverted structures. Specifically, decreasing the number of alkyl and alkoxy groups in the molecular structure of SSO in series SSO3-SSO2-SSO1 increases the SSO:$PC_{71}BM$ ratio on the top of the active layer indicating that the inverted structure is preferential for SSO1. We propose that the observed correlations can be associated to a vertical phase separation of the donor and acceptor phases in the active layer.

Acknowledgements

This work in part of materials synthesis and characterization was supported by Russian Science Foundation (grant 14-13-01380). This work was done using equipment purchased under the Lomonosov Moscow State University Program of Development. Device fabrication performed at Cyprus University of Technology. S.A.C. and V.A.T. would like to acknowledge networking and short-term scientific missions support respectively by the COST Action MP1307.

Appendix A. Supplementary data

Supplementary data associated with this article can be found, in the online version, at http://dx.doi.org/10.1016/j.synthmet.2016.02.022.

References

[1] Y. Lin, Y. Li, X. Zhan, Small molecule semiconductors for high-efficiency organic photovoltaics, Chem. Soc. Rev. 41 (2012) 4245–4272.
[2] Heliatek consolidates its technology leadership by establishing a new world record for organic solar technology with a cell efficiency of 12%. Dresden, Germany, (2013).
[3] J. Roncali, Molecular bulk heterojunctions: an emerging approach to organic solar cells, Acc. Chem. Res. 42 (2009) 1719–1730.
[4] J. Zhang, D. Deng, C. He, Y. He, M. Zhang, Z.-G. Zhang, Z. Zhang, Y. Li, Solution-processable star-shaped molecules with triphenylamine core and dicyanovinyl endgroups for organic solar cells, Chem. Mater. 23 (2011) 817–822.
[5] J. Min, Y.N. Luponosov, T. Ameri, A. Elschner, S.M. Peregudova, D. Baran, T. Heumueller, N. Li, F. Machui, S. Ponomarenko, C.J. Brabec, A solution-processable star-shaped molecule for high-performance organic solar cells via alkyl chain engineering and solvent additive, Org. Electron. 14 (2013) 219–229.
[6] J. Min, Y.N. Luponosov, A. Gerl, M.S. Polinskaya, S.M. Peregudova, P.V. Dmitryakov, A.V. Bakirov, M.A. Shcherbina, S.N. Chvalun, S. Grigorian, N. Kaush-Busies, S.A. Ponomarenko, T. Ameri, C.J. Brabec, Alkyl chain engineering of solution-processable star-shaped molecules for high-performance organic solar cells, Adv. Energy Mater. 4 (2013), doi:http://dx.doi.org/10.1002/aenm.201301234.
[7] S.A. Ponomarenko, Y.N. Luponosov, J. Min, A.N. Solodukhin, N.M. Surin, M.A. Shcherbina, S.N. Chvalun, T. Ameri, C. Brabec, Design of donor-acceptor star-shaped oligomers for efficient solution-processible organic photovoltaics, Faraday Discuss. 174 (2014) 313–339.
[8] J. Min, Y.N. Luponosov, Z.-G. Zhang, S.A. Ponomarenko, T. Ameri, Y. Li, C.J. Brabec, Interface design to improve the performance and stability of solution-processed small-molecule conventional solar cells, Adv. Energy Mater. 4 (2014) 1400816.
[9] G. Li, C.-W. Chu, V. Shrotriya, J. Huang, Y. Yang, Efficient inverted polymer solar cells, Appl. Phys. Lett. 88 (2006) 253503.
[10] M. Jorgensen, K. Norrman, S.A. Gevorgyan, T. Tromholt, B. Andreasen, F.C. Krebs, Stability of polymer solar cells, Adv. Mater. 24 (2012) 580–612.
[11] A.K.K. Kyaw, D.H. Wang, V. Gupta, J. Zhang, S. Chand, G.C. Bazan, A.J. Heeger, Efficient solution-processed small-molecule solar cells with inverted structure, Adv. Mater. 25 (2013) 2397–2402.
[12] A. Savva, F. Petraki, P. Elefteriou, L. Sygellou, M. Voigt, M. Giannouli, S. Kennou, J. Nelson, D.D.C. Bradley, C.J. Brabec, S.A. Choulis, The effect of organic and metal oxide interfacial layers on the performance of inverted organic photovoltaics, Adv. Energy Mater. 3 (2013) 391–398.
[13] C. Waldauf, M. Morana, P. Denk, P. Schilinsky, K. Coakley, S.A. Choulis, C.J. Brabec, Highly efficient inverted organic photovoltaics using solution based titanium oxide as electron selective contact, Appl. Phys. Lett. 89 (2006) 233517.
[14] J. Min, H. Zhang, T. Stubhan, Y.N. Luponosov, M. Kraft, S.A. Ponomarenko, T. Ameri, U. Scherf, C.J. Brabec, A combination of Al-doped ZnO and a conjugated polyelectrolyte interlayer for small molecule solution-processed solar cells with an inverted structure, J. Mater. Chem. A 1 (2013) 11306–11311.

[15] I. Burgués-Ceballos, F. Machui, J. Min, T. Ameri, M.M. Voigt, Y.N. Luponosov, S.A. Ponomarenko, P.D. Lacharmoise, M. Campoy-Quiles, C.J. Brabec, Solubility based identification of green solvents for small molecule organic solar cells, Adv. Funct. Mater. 24 (2014) 1449–1457.
[16] J. Min, Y.N. Luponosov, A.N. Solodukhin, N. Kausch-Busies, S.A. Ponomarenko, T. Ameri, C.J. Brabec, A star-shaped D-π-A small molecule based on a tris(2-methoxyphenyl)amine core for highly efficient solution-processed organic solar cells, J. Mater. Chem. C 2 (2014) 7614–7620.
[17] Y.N. Luponosov, J. Min, A.N. Solodukhin, A.V. Bakirov, P.V. Dmitryakov, M.A. Shcherbina, S.M. Peregudova, G.V. Cherkaev, S.N. Chvalun, C.J. Brabec, S.A. Ponomarenko, Star-shaped D-π-A oligothiophenes with tris(2-methoxyphenyl) amine core and alkyldicyanovinyl groups: synthesis, structural, photophysical, and photovoltaic properties, (2016) (submitted for publication).
[18] A. Savva, S.A. Choulis, Cesium-doped zinc oxide as electron selective contact in inverted organic photovoltaics, Appl. Phys. Lett. 102 (2013) 233301.
[19] S.R. Hammond, J. Meyer, N.E. Widjonarko, P.F. Ndione, A.K. Sigdel, A. Garcia, A. Miedaner, M.T. Lloyd, A. Kahn, D.S. Ginley, J.J. Berrya, D.C. Olsona, Low-temperature, solution-processed molybdenum oxide hole-collection layer for organic photovoltaics, J. Mater. Chem. 22 (2012) 3249–3254.
[20] A.M. Nardes, M. Kemerink, M.M. de Kok, E. Vinken, K. Maturova, R.A.J. Janssen, Conductivity, work function, and environmental stability of PEDOT:PSS thin films treated with sorbitol, Org. Electron. 9 (2008) 727–734.